

# Phase mapping for cardiac unipolar electrograms with neural network instead of phase transformation

Konstantin Ushenin  
Institute of Natural Sciences  
Ural Federal University  
Ekaterinburg, Russia  
konstantin.ushenin@urfu.ru

Tatyana Nesterova  
Laboratory of Mathematical Physiology  
Institute of Immunology and Physiology  
Ekaterinburg, Russia  
tatiannesterova@gmail.com

Dmitry Smarko  
Laboratory of Mathematical Physiology  
Institute of Immunology and Physiology  
Ekaterinburg, Russia  
d.shmarko@yandex.ru

Vladimir Sholokhov  
Institute of Natural Sciences  
Ural Federal University  
Ekaterinburg, Russia  
vdsholokhov@yandex.ru

**Abstract**—A phase mapping is an approach to processing signals of electrograms recorded from the surface of cardiac tissue. The main concept of phase mapping is the application of the phase transformation with the aim to obtain signals with useful properties. In our study, we propose to use a simple sawtooth signal instead of a phase signal for processing of electrogram data and building of the phase maps. We denote transformation that can provide this signal as a phase-like transformation (PLT). PLT defined via a convolutional neural network that is trained on a dataset from computer models of cardiac tissue electrophysiology. The proposed approaches were validated on data from the detailed personalized model of the human torso electrophysiology. This paper includes visualization of the phase map based on PLT and shows the robustness of the proposed approaches in the analysis of the complex non-stationary periodic activity of the excitable cardiac tissue.

**Index Terms**—digital signal processing, neural network, convolutional neural network, unipolar electrogram, cardiac mapping, phase mapping, cardiology, electrophysiological study

## I. INTRODUCTION

A unipolar electrogram is a widespread method for invasive electrophysiological studies in cardio-surgery [1]. Cardiac mapping is a modern extension of a unipolar electrogram analysis that presents cardiac electrophysiology in the format of maps or video maps.

The most complex processing is required for the presentation of the periodic and non-stationary periodic activity of myocardium (cardiac muscle tissue). This activity usually observed during the ventricular tachycardia or atrial flutter. A phase mapping is the most common approach for processing of such type of data. These approaches were widely used in biological in vitro experiments [2]–[4], and lately was translated to clinical practice [5]–[7].

The phase mapping approach includes two parts. The first part is the phase transformation of the signals that are recorded

The reported study was funded by RFBR according to the research project No. 18-31-00401. Development of the mathematical models are supported by IIF UrB RAS theme #AAAA-A18-118020590031-8, RF Government Act #211 of March 16, 2013, the Program of the Presidium RAS.

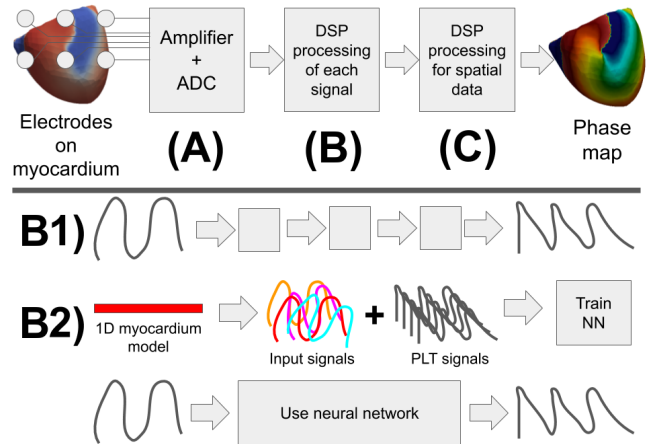


Fig. 1. The main idea of the current paper. A phase mapping is an approach to process data from unipolar electrodes placed on the myocardium. It is shown on the top row (A,B,C). Some parts of the phase mapping require the processing of signals from each electrode (B). The signal processing pipeline here is usually a sequence of mathematical transformations (B1). We propose to use a computer model of a 1D myocardial strand for the generation of training datasets for the neural networks (B2). The trained neural network can replace all steps of the pipeline. Abbreviations: analog-to-digital converter (ADC), digital signal processing (DSP), Neural network (NN).

from several leads, and the second part is an interpolation and spatial analysis of all phase signals (see Fig. 1). The phase transformation usually based on a shift in time or Hilbert transform [7]. Also, several alternative approaches were proposed [5].

Here, we are aiming to replace the phase transformation on the more robust approach. We propose to use a sawtooth signal with [0,1] range of values. These signals should have breaks that related to depolarization of transmembrane potential in cardiomyocytes in point of measurements. Between to depolarization, the excitation signal should linearly be reduced from 1 to 0 value. Fig. 2 shows the proposed signal and its relationship with the cardiomyocyte transmembrane potential.

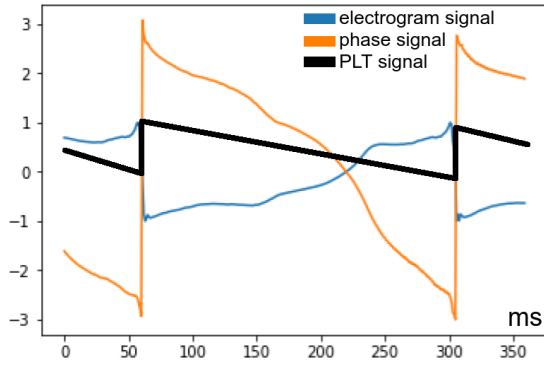


Fig. 2. Explanation of phase-like transformation (PLT). In phase map processing, the original electrogram signal (blue line; visualized after normalization) is transformed to the phase signal (orange line). We propose to use the sawtooth signal (black line) that has basic properties of phase signal but is significantly simpler.

This signal should be obtained from unipolar electrogram with some transformation. We named this transformation as the phase-like transformation (PLT). In contradiction to previously proposed approaches [2]–[7] we do not define this transformation as series of mathematical operations (see Fig. 1(A1)). We define the PLT via training of neural network on series of simple 1D model of myocardial electrophysiology (see Fig. 1(A2)).

For proof-of-concept, we test the proposed idea with the more complex and detailed model of the human heart electrophysiology.

## II. METHODS

*Idealized 1D models of myocardial tissue* were computed with monodomain equation [8]. The 1D strand contained 1024 points and the activation point was located in 128 nodes from one side of the strands. Courtenance98 [9] and TNNP06 [10] described electrophysiological activity of atrial and ventricular cardiomyocytes respectively.

*Unipolar electrograms from 1D strand* were obtained with the following formula [11]:

$$\phi(x') = -\kappa \int_x \frac{\partial V}{\partial x} \cdot \frac{\partial}{\partial x} \left( \frac{1}{\sqrt{(x-x')^2 + h^2}} \right) dx \quad (1)$$

where  $V$  is the transmembrane potential in point  $x$ ,  $\phi$  is an extracellular potential or signal from a unipolar catheter,  $h$  is the height of the catheter above the 1D strand, and  $x'$  is an electrode position.

The coefficient  $\kappa$  and a voltage in absolute physical values are not important for our study because we normalized results using the division of each signal to their maximal absolute amplitude.

*Training and validation datasets were generated* with a variation of the following model parameters: the stimulation frequency ( $FR = \{2000, 1000, 500, 300, 200\}$  Hz), conduction velocity ( $CV = \{10, 20, 40, 80\}$ ), height of electrode over the strand ( $h = \{5, 10, 20, 50, 80\}$ ) and position of

electrode along the strand ( $x' = \{448, 512, 640\}$ ). Generation of dataset for the atrial and ventricular dataset were separated. Parameters of the cardiomyocytes were taken from the original articles [9], [10] without changes. PLT signals for training were computed with simple heuristic algorithms in accordance with the moment of time when the action potential crossed the 0 mV threshold level. Examples of PTL signals are shown in Figure 3. Thus, the full datasets of simple model results contained 300 signals with 4096 ms lengths and 1000 Hz frequency of discretization. The training and validation datasets respectively contain 150 (50%) and 150 (50%) signals.

*The test dataset* was generated by a detailed personalized finite element model of two ventricles and the torso. Model geometry was based on computed tomography data of one patient. The torso includes regions of the heart, lungs, blood in heart chambers, and spinal cord. Each torso region had realistic conductivity, according to [12]. The heart included realistic conduction anisotropy that was introduced with a rule-based approach [13] and realistic heterogeneity of current transmembrane densities [14]. The TNNP06 model [10] performed a realistic simulation of cardiomyocytes electrophysiology. A bidomain model with bath described excitation wave propagation and the torso electrophysiology. We initiate a spiral wave using the S1S2 protocol to provide realistic extracellular potential for ventricular arrhythmia of the reentry type. Each point of the heart surface mesh provides one signal for the test dataset. Thus, the entire model provides 34354 signals with 4096 ms length.

The described approach is one of the most realistic ways for the simulation of electrophysiology in both ventricles and the torso. In particular, this approach correctly includes the far-field effect. The used model was verified against clinical data of electrocardiography with 224 leads during activation of the myocardium from a point [15]. We suppose that model complexity and a wide representation of physiological features make the model suitable for the generation of the test dataset. This dataset were used only with the neural network that is trained to process of the signals from the ventricular myocardium.

*Convolutional neural network for processing* was adapted from U-Net architecture for biomedical image segmentation [16]. NN takes the signal of the electrogram as an image with a height of 1 px and a width of 4096 px. All convolution kernels, pooling, and upsampling windows were replaced from 3x3 size to 3x1 size. The number of neurons in all layers was proportionally increased for the processing of vectors with a 4096 element size. The size of the pooling layers was replaced from 2x2 to 4x1 with an aim to increase the perception field of NN. Furthermore, we add Dropout (30%) and Gaussian noise layer (mean=0, std.=0.2) before the U-Net narrow layer for improving NN robustness to white noise. The loss function was a sum of the mean absolute error and mean squared error with equal weights. We used the ADAM method of optimization with learning rate reduction on plateau of validation loss. NN provides a PLT signal as an output.

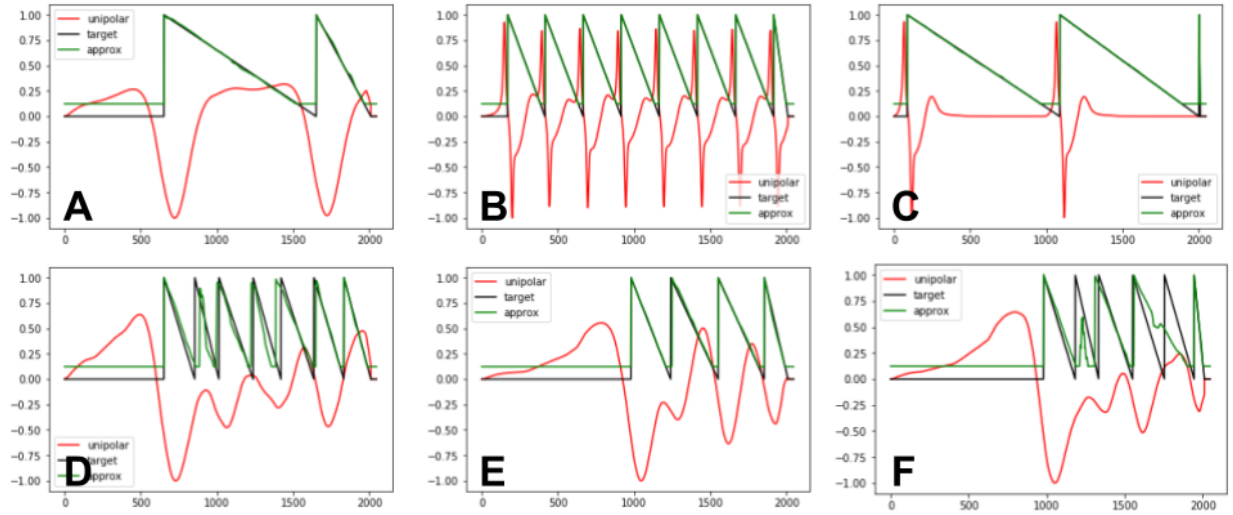


Fig. 3. Examples of electrogram signals, target PLT signals and PLT signals provided as output of the neural network. The top row (A,B,C) shows a signal for periodic activation of the strand, and the bottom row (D,E,F) shows signals for strand activation on high frequency, which causes action potential alternations. Cases A,B,C,D,E were correctly processed by neural network, and case F includes artifacts.

### III. RESULTS

The model of cardiac tissue provides a set of excitation waves for a normal healthy myocardium (Fig. 3(A-B)) and additionally provide cases with the action potential alternances (Fig. 3(D-F)). The last ones appeared under high stimulation frequency at the 1D strand of atrial tissue (Courtenance98 model [9]).

Idealized models provide a set of unipolar electrograms with significant differences between cases. The majority of signals were similar to clinically observed electrophysiological behaviour for sino-atrial rhythm (Figure 3(A,C), [1]), atrial flutter and atrial fibrillation (Figure 3(B,D-F), [17]). However, some signals look atypical, and we suppose that the dataset covers both real and unobtainable cases of electrogram signals.

	Num. of cases	Atriums		Ventricles	
		MAE	MSE	MAE	MSE
Train (1D)	150	0.0248	0.0023	0.0250	0.0021
Validation (1D)	150	0.0289	0.0040	0.0327	0.0024
Test (3D)	34354	-	-	0.0888	0.0266

TABLE I

METRICS OF NEURAL NETWORK PERFORMANCE AT 150 EPOCH. MEAN ABSOLUTE ERROR (MAE), MEAN SQUARE ERROR (MSE).

NN training requires 100+ epochs for reaching of a loss plateau. Figure ?? and Table I shows the training process and final value of loss respectively. We manually analyzed shapes of the sawtooth signals and counted a number of wrongly detected action potential upstrokes in the validation dataset. Only 10 out of 859 (1.16%) upstrokes were incorrectly detected.

Qualitative analysis of NN outputs are presented in Figure 3. NN perfectly processes any periodic signals and the major part of non-stationary periodic signals (see 3(A-E)). However, the model makes an error with some non-stationary periodic signals that contain double peaks with close placement (see

3(F)). The model cannot reach zero levels in zones without electrophysiological activity and in the ends of the sawtooth shapes.

The result of the NN application on the realistic personalized model of human electrophysiology is presented in Figure 4. There are extracellular potential, transmembrane potential and phase map based on the proposed signal processing approach. As can be seen, the obtained quality of the phase map clearly reveals the rotor core and the front of the excitation waves. However, the value of the mean absolute error metric here is at three and half times higher than the ones for 1D strand models (see Table I).

### IV. DISCUSSION AND CONCLUSION

In our study, we propose phase-like transformation (PLT) for processing unipolar electrograms and the method of its definition via the convolutional neural network that is trained on a set of generated data from the numerical experiments.

The proposed transformation provides signals with desirable properties as we planned in the beginning. It can reveal complex non-stationary periodic behavior in the myocardium and is applicable for the building of phase maps (see Fig. 4).

Our approach to transformation definition significantly differs from the method that was proposed before. It does not require a manual choice of signal transformations and filters with good basic properties. Instead of that, they require proper choice and tuning of several models of the physiological process. Loss functions here is a direct way for assessment of the algorithm able to process complex data.

We suppose that the proposed approach has a wide area of application. It may be applied to the processing of unipolar electrograms from the unipolar catheter, multi-leads catheter, and balloons, microelectrode arrays, invasive and non-invasive systems of cardiac mapping [18], [19].

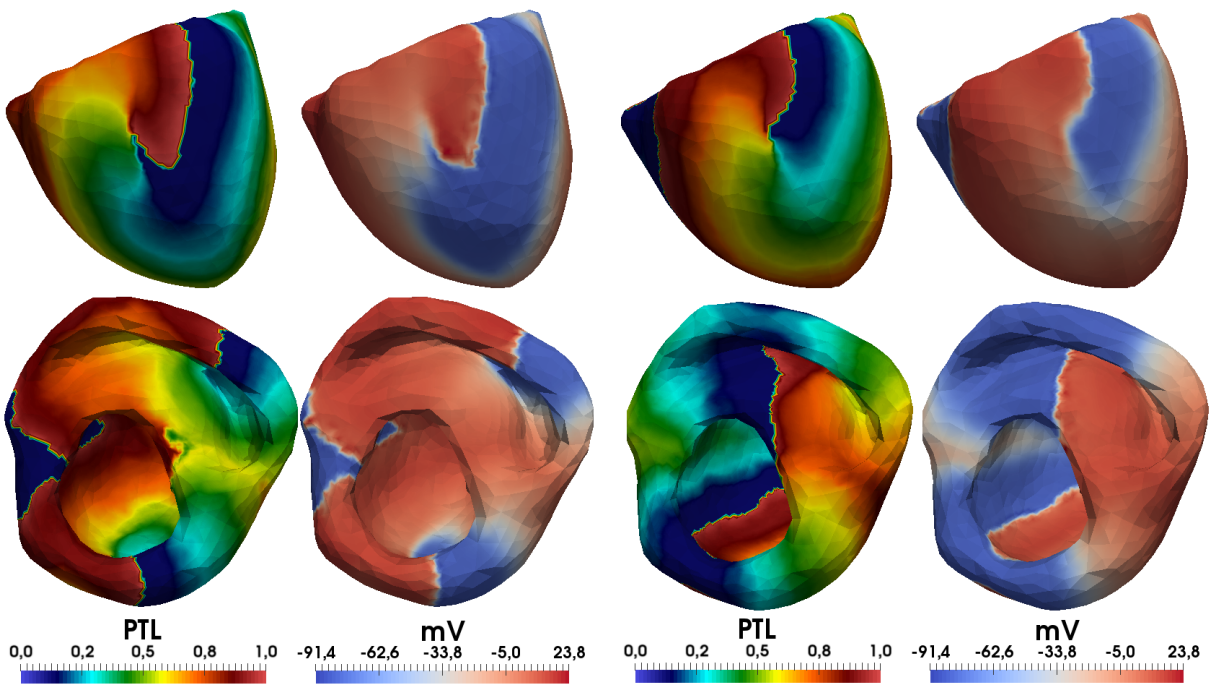


Fig. 4. Phase maps based on PLT signals and action potential in a fixed moment of time. Data was obtained in the detailed computer model of the ventricular tachycardia.

#### REFERENCES

- [1] U. B. Tedrow and W. G. Stevenson, "Recording and interpreting unipolar electrograms to guide catheter ablation," *Heart Rhythm*, vol. 8, no. 5, pp. 791–796, 2011.
- [2] M.-A. Bray and J. P. Wikswo, "Considerations in phase plane analysis for nonstationary reentrant cardiac behavior," *Physical Review E*, vol. 65, no. 5, p. 051902, 2002.
- [3] M. P. Nash, A. Mourad, R. H. Clayton, P. M. Sutton, C. P. Bradley, M. Hayward, D. J. Paterson, and P. Taggart, "Evidence for multiple mechanisms in human ventricular fibrillation," *Circulation*, vol. 114, no. 6, pp. 536–542, 2006.
- [4] K. Umopathy, K. Nair, S. Masse, S. Krishnan, J. Rogers, M. P. Nash, and K. Nanthakumar, "Phase mapping of cardiac fibrillation," *Circulation: Arrhythmia and Electrophysiology*, vol. 3, no. 1, pp. 105–114, 2010.
- [5] P. Kuklik, S. Zeemering, B. Maesen, J. Maessen, H. J. Crijns, S. Verheule, A. N. Ganesan, and U. Schotten, "Reconstruction of instantaneous phase of unipolar atrial contact electrogram using a concept of sinusoidal recomposition and hilbert transform," *IEEE transactions on biomedical engineering*, vol. 62, no. 1, pp. 296–302, 2015.
- [6] R. Vijayakumar, S. K. Vasireddi, P. S. Cuculich, M. N. Faddis, and Y. Rudy, "Methodology considerations in phase mapping of human cardiac arrhythmias," *Circulation: Arrhythmia and Electrophysiology*, vol. 9, no. 11, p. e004409, 2016.
- [7] R. Dubois, A. Pashaei, J. Duchateau, and E. Vigmond, "Electrocardiographic imaging and phase mapping approach for atrial fibrillation: A simulation study," in *Computing in Cardiology Conference (CinC), 2016*. IEEE, 2016, pp. 117–120.
- [8] J. Keener and J. Sneyd, *Mathematical physiology 1: Cellular physiology*. Springer, 2009, vol. 2.
- [9] M. Courtemanche, R. J. Ramirez, and S. Nattel, "Ionic mechanisms underlying human atrial action potential properties: insights from a mathematical model," *American Journal of Physiology-Heart and Circulatory Physiology*, vol. 275, no. 1, pp. H301–H321, 1998.
- [10] K. H. Ten Tusscher and A. V. Panfilov, "Alternans and spiral breakup in a human ventricular tissue model," *American Journal of Physiology-Heart and Circulatory Physiology*, vol. 291, no. 3, pp. H1088–H1100, 2006.
- [11] S. Weinberg, S. Irvanian, and L. Tung, "Representation of collective electrical behavior of cardiac cell sheets," *Biophysical journal*, vol. 95, no. 3, pp. 1138–1150, 2008.
- [12] D. U. Keller, F. M. Weber, G. Seemann, and O. Dossel, "Ranking the influence of tissue conductivities on forward-calculated ecgs," *IEEE Transactions on Biomedical Engineering*, vol. 57, no. 7, pp. 1568–1576, 2010.
- [13] J. Bayer, R. Blake, G. Plank, and N. Trayanova, "A novel rule-based algorithm for assigning myocardial fiber orientation to computational heart models," *Annals of biomedical engineering*, vol. 40, no. 10, pp. 2243–2254, 2012.
- [14] D. U. Keller, D. L. Weiss, O. Dossel, and G. Seemann, "Influence of  $i_{K_s}$  heterogeneities on the genesis of the t-wave: A computational evaluation," *IEEE Transactions on Biomedical Engineering*, vol. 59, no. 2, pp. 311–322, 2012.
- [15] K. S. Ushenin, A. Dokuchaev, S. M. Magomedova, O. V. Sopov, V. V. Kalinin, O. Solovyova, and E. S. SA, "Role of myocardial properties and pacing lead location on ecg in personalized paced heart models," *Age*, vol. 67, p. 56, 2018.
- [16] O. Ronneberger, P. Fischer, and T. Brox, "U-net: Convolutional networks for biomedical image segmentation," in *International Conference on Medical image computing and computer-assisted intervention*. Springer, 2015, pp. 234–241.
- [17] K. T. Konings, J. L. Smeets, O. C. Penn, H. J. Wellens, and M. A. Allessie, "Configuration of unipolar atrial electrograms during electrically induced atrial fibrillation in humans," *Circulation*, vol. 95, no. 5, pp. 1231–1241, 1997.
- [18] A. Kalinin, D. Potyagaylo, and V. Kalinin, "Solving the inverse problem of electrocardiography on the endocardium using a single layer source," *Frontiers in physiology*, vol. 10, p. 58, 2019.
- [19] A. S. Revishvili, E. Wissner, D. S. Lebedev, C. Lemes, S. Deiss, A. Metzner, V. V. Kalinin, O. V. Sopov, E. Z. Labartkava, A. V. Kalinin *et al.*, "Validation of the mapping accuracy of a novel non-invasive epicardial and endocardial electrophysiology system," *Europace*, p. euu339, 2015.